

For $S=8R_p=5000 \text{ \AA}$ and the same values of D and M_s , it can be shown that $\Delta H \sim 4\pi M_s n^2$ for a small range of n around $n \cong 15$. The mode n scatters only into modes nearby in \mathbf{k} space in this case, and the factor $n^2 \sim k_n^2$ is the usual density-of-states factor.

In order to determine if the present model is valid, it would be necessary to inspect the film to determine the size $2R_p$ of the scattering centers and the packing factor f . In the absence of this information, it can be stated only that the results afford a possible explanation of several experimental results. For example, Phillips and Rosenberg¹⁴ and Wigen¹⁵ have reported

¹⁴ T. G. Phillips and H. M. Rosenberg, Phys. Letters **8**, 298 (1964).

¹⁵ P. E. Wigen, Phys. Rev. **133**, A1557 (1964).

$\Delta H \sim n^2$ for modes with $11 \leq n \leq 21$ in a Co film and for $\sim 4 \leq n \leq 9$ in a permalloy film, respectively. Two of the cases above give $\Delta H \sim n^2$ with the correct order of magnitude ($\Delta H \sim 100$ Oe for the large- n modes). Weber, Tannenwald, and Bajorek¹⁶ have observed linewidths independent of n for large values of n ($9 \leq n \leq n_{\max}$, where n_{\max} ranged from 15 to 31). For $n=9$, the value of Dk_{nz}^2 is ~ 1600 Oe, which is considerably smaller than $2\pi M_s=5500$ Oe. Although the present results predict that ΔH is independent of n for large n , they cannot explain the fact that ΔH is independent of n for the smaller values of n .

¹⁶ R. Webber, P. E. Tannenwald, and C. Bajorek (unpublished).

Ferromagnetic Resonance in Thin Films. III. Theory of Mode Intensities

M. SPARKS*

Science Center, North American Rockwell Corporation, Thousand Oaks, California 91360

(Received 18 August 1969)

A theory of surface-spin pinning and its effects on the ferromagnetic-resonance mode intensities is presented. The pinning by a surface inhomogeneity (e.g., a demagnetization field from surface imperfections or an inhomogeneous saturation magnetization) of thickness ϵ is considered. Roughly speaking, the modes are nearly unpinned for a thin-surface inhomogeneity ($\epsilon^2 \ll \Lambda/\pi$, where Λ is the exchange constant in the exchange field $\Lambda \nabla^2 \mathbf{M}$), while the low-order modes are pinned by a thick-surface inhomogeneity ($\epsilon^2 \gg \Lambda/\pi$ not satisfied). The theory indicates that the low-order modes should be pinned unless great care is exercised in the film preparation. In 80% Ni-20% Fe permalloy, $(\Lambda/\pi)^{1/2} \cong 90 \text{ \AA}$; thus, the surface region would have to be only a few lattice constants thick in order for there to be no pinning. These results are obtained by considering the equation of motion of the magnetization in the surface region as well as the bulk region. The intensities and frequencies of magnetostatic modes (negligible exchange energy) are relatively independent of surface-spin pinning, in contrast to the result for exchange modes (negligible microwave demagnetization energy) that pinning the surface spins gives rise to large intensities of even modes.

I. INTRODUCTION

SINCE Kittel's suggestion¹ in 1958 that the exchange integral in ferromagnetic materials could be obtained by ferromagnetic-resonance measurements in thin films, interest in this field has increased steadily.¹⁻⁵

* Present address: The RAND Corp., Santa Monica, Calif.

¹ C. Kittel, Phys. Rev. **110**, 1295 (1958); C. F. Kooi, Phys. Rev. Letters **20**, 450 (1968); G. I. Lykken, *ibid.* **19**, 1431 (1967); T. G. Phillips, Proc. Roy. Soc. (London), **A292**, 224 (1966); R. F. Soohoo, *Magnetic Thin Films* (Harper and Row, New York, 1965); R. Weber and P. E. Tannenwald, Phys. Rev. **140**, A498 (1965); P. Pincus, *ibid.* **118**, 658 (1960); M. H. Seavey, Jr., and P. E. Tannenwald, Phys. Rev. Letters, **1**, 168 (1958); H. S. Jarrett and R. K. Waring, Phys. Rev. **111**, 1223 (1958); Z. Frait and M. Ondris, Czech. J. Phys. **B11**, 463 (1961); L. Néel, J. Phys. Radium **15**, 15 (1954); M. Nisenoff and R. W. Terhune, J. Appl. Phys. **36**, 732 (1965).

² G. T. Rado and J. R. Weertman, J. Phys. Chem. Solids **11**, 315 (1959).

³ A. M. Portis, Appl. Phys. Letters **2**, 69 (1963).

⁴ C. F. Kooi, P. E. Wigen, M. R. Shanabarger, and J. V. Kerrigan, J. Appl. Phys. **35**, 791 (1964); P. E. Wigen, C. F. Kooi, and M. R. Shanabarger, *ibid.* **35**, 3302 (1964); E. Hirota, J. Phys. Soc. Japan **19**, 1 (1964).

Interpretation of experimental results has been obscured by a lack of understanding of the boundary conditions⁶ at the film surfaces. The theories of Wigen, Kooi, and co-workers⁴ (saturation magnetization M_z of surface layer different from that of the bulk) and Portis³ (parabolic M_z) explain the positions and critical-angle depinning, but not the intensities, of exchange modes.^{6a} Rado and Weertman² have shown that in the absence of a specific mechanism to pin⁶ the surface spins, the exchange interaction makes the normal derivative of the magnetization zero for the long-wavelength modes. Thus, the intensities of all long-wavelength modes except the main-branch modes^{6a} are zero in this case.

⁵ P. E. Wigen, C. F. Kooi, M. R. Shanabarger, and T. D. Rossing, Phys. Rev. Letters **9**, 206 (1962).

⁶ The surface spins are said to be *pinned* (or *unpinned*) if the microwave magnetization m is zero [or $dm/dz' = 0$] at the surface. See the discussion of (1.4) in the text.

^{6a} Exchange modes have negligible microwave demagnetization energy, and magnetostatic modes have negligible exchange energy. The main-branch modes have the smallest value of k_z' , where \hat{z}' is the film normal.

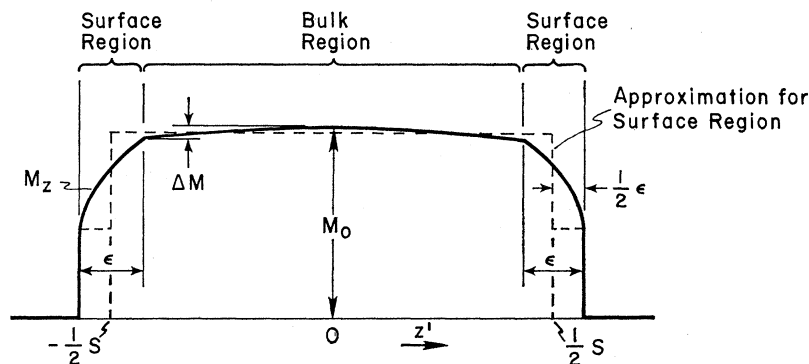


FIG. 1. Variation of the saturation magnetization M_z across the thickness (z' axis) of the film.

A theory of surface-spin pinning⁶ is developed to explain the mode intensities. The theory, which applies to exchange and magnetostatic modes, both bulk and surface types, is based on a physical model which is essentially a composite of the Wigen-Kooi⁴ and Portis³ models. The magnetization can be written as

$$\mathbf{M} = \hat{z}M_z + \mathbf{m}, \quad (1.1)$$

where the transverse microwave magnetization \mathbf{m} is orthogonal to the unit vector \hat{z} . The saturation magnetization⁷ M_z is assumed to vary across the thickness of the film as illustrated in Fig. 1. Note that the z' axis is perpendicular to the plane of the film, while the equilibrium position of \mathbf{M} is along \hat{z} .

In the surface region of thickness ϵ , which is assumed to be much smaller than the film thickness S , M_z drops off from its bulk value to zero, and, in the bulk region, M_z is a function of z' :

$$M_z = M_0 - \Delta M f(z'). \quad (1.2)$$

Portis³ considered the case of $f(z') = (2z'/S)^2$ and perpendicular resonance.⁸ His theory applies to the frequencies and intensities of the low-order modes (with exchange energy $\lesssim 2\pi\hbar|\gamma|\Delta M$), which are said to be "in the Portis well." We shall restrict our attention to the modes out of the Portis well (exchange energy $\lesssim 2\pi\hbar|\gamma|\Delta M$).

The saturation magnetization and internal field H_i may have the same spatial variation across the thickness of the sample; however, this is not the case, in general. For example, the demagnetization field from a rough sample surface can cause M_z and H_i to have quite different spatial dependences.⁹ In the bulk region,

$$H_i = H_{i0} + \Delta H_i g(z'). \quad (1.3)$$

Possible sources of the inhomogeneities in M_z and H_i are surface imperfections,⁹ a fractional density of oxide

⁷ We make the linearization approximation that the z component M_z of \mathbf{M} is approximately equal to the saturation magnetization. In the present paper, the saturation magnetization is written as M_z .

⁸ Perpendicular (or parallel) resonance denotes that the applied field is perpendicular (or parallel) to the film surface.

⁹ M. Sparks, Part IV of the present series of papers (unpublished).

which increases as the surface is approached,³ inhomogeneous local strains,⁹ or perhaps other sources. Note that a *constant* stress at the film-substrate interface gives an extremely small gradation in the strain across the thickness of a thin film.¹⁰

By considering the equations of motion of the microwave magnetization \mathbf{m} in the surface region as well as in the bulk region, the following results are obtained: Roughly speaking the exchange interaction tries to make $d\mathbf{m}/dz' = 0$, while a surface layer of different M_z or H_i tries to make $\mathbf{m} = 0$. If $\epsilon = \Delta M = 0$, the surface spins are unpinned for the long-wavelength modes. This result,² which is derived from the equations of motion in the Appendix, also can be obtained by considering the torques on the spins in the neighborhood of the sharp surface. A spin at the surface and one directly in from the surface must have the same value of \mathbf{m} , since all spins must precess at the same frequency in a normal mode and a nonzero slope of \mathbf{m} would give an extra torque on the surface spin because of the missing neighbors. The short-wavelength modes are unpinned for some crystals and surfaces, but not for others. Changing an exchange integral or anisotropy energy at the surface can give modes which are not unpinned.

For $\Delta M = 0$ and $\epsilon \neq 0$, it will be shown that the surface spins will remain unpinned for $\epsilon^2 \ll \epsilon_{cr}^2$. The value of the critical thickness ϵ_{cr} is typically of the order of $(\Lambda/\pi)^{1/2}$ for perpendicular resonance, where Λ is the exchange constant [see Eq. (2.1)]. For 80% Ni-20% Fe permalloy, $\sqrt{\Lambda} = 160 \text{ \AA}$, and for yttrium iron garnet (YIG), $\sqrt{\Lambda} = 568 \text{ \AA}$.

If $\epsilon^2 \ll \epsilon_{cr}^2$ is *not* satisfied, the surface exchange cannot hold $d\mathbf{m}/dz' = 0$ at the surface. The low-order modes are then pinned since the spins in the surface region are "off resonance" when the spins in the bulk region are "on resonance" and the surface spins are exchange and dipole coupled to the bulk spins. However, the higher-order modes are only partially pinned, as will be shown. In order to satisfy $\epsilon^2 \ll \epsilon_{cr}^2$ with $\epsilon_{cr} \cong (\Lambda/\pi)^{1/2} \cong 90 \text{ \AA}$, the surface region would have to be only a few lattice constants thick in permalloy films. Since extreme care would be required to fabricate such films, it is expected

¹⁰ B. J. Aleck, J. Appl. Mechanics **16**, 118 (1949).

that there will be pinning in these films unless great care is exercised in the film preparation.

In the past, the mode intensities have been related to a fixed pinning condition at the film surface, such as²

$$am + b \frac{dm}{dz'} = 0. \quad (1.4)$$

This concept of pinning is not valid, strictly speaking, for several reasons.¹¹ First, the true boundary conditions are those which the field must satisfy at infinity; certain continuity conditions must be satisfied at the sample surfaces. Here, the condition (1.4) will be called a *pinning condition*, to distinguish it from the usual boundary conditions. Second, the pinning condition is a dynamic one, which varies with mode number, frequency, etc., as discussed below, not a fixed one such as (1.4). Third, the surface of the sample cannot be considered as a mathematical plane, but must be considered as a region of finite thickness, in general, and the intensities depend upon the value of \mathbf{m} in the surface region as well as in the bulk region. Fourth, even if the pinning conditions (1.4) were known for a given case, the intensity of the mode could not be determined unless \mathbf{m} were a single cosine function, which is not true in general for two reasons: When H_i is not constant, \mathbf{m} will not be a cosine function. Even when H_i is constant, a single cosine function is not sufficient to describe \mathbf{m} properly when both exchange and demagnetization energies are included. Benson and Mills¹² have shown that a rounding of m near the surface to make the normal derivative zero is important. It is easy to show that this rounding can be accomplished by adding a rapidly decaying exponential function to \mathbf{m} (as well as by the "1-x²"-type rounding used by Benson and Mills), thus, giving a two-wave-vector expression for \mathbf{m} . Gann¹³ has shown that three wave vectors are required in the long-wavelength limit, in general, when both exchange and demagnetization are included.

As discussed in Sec. 9 of Paper I in the present series,¹¹ an important consequence of including the exchange interaction in the calculation of ω and \mathbf{m} for magnetostatic modes is that the frequencies and intensities of *magnetostatic modes* are relatively insensitive to the amount of explicit surface-spin pinning. The reason is as follows: Typically one of the three waves of Gann¹³ is negligible, and one is approximately the same as the wave for a pure magnetostatic mode ($\Lambda=0$ and no explicit pinning mechanism). The third wave is either rapidly oscillating or rapidly decaying. Waves two and three are added together to satisfy the given pinning condition. The addition of the third wave does not change the intensity since it integrates to zero approxi-

mately, and it does not change the frequency since it has the same frequency as the second wave.

The intensities of the exchange modes are of course closely related to the pinning. The *intensity* calculations in Secs. 4-8 apply to exchange modes since they are essentially single-wave calculations. The considerations of the pinning by the surface layer can be applied to the magnetostatic modes with very little modification. A surface layer is expected to pin both the exchange and magnetostatic modes, but the pinning effects the intensities of the exchange modes but not of the magnetostatic modes.

The following assumptions will be made. The effects of eddy currents are neglected. If the skin depth is less than the film thickness, then Eq. (4.1) for the intensities must be modified. A shape factor describing the penetration of the microwave field could be added to (4.1). The wave-vector components in the plane of the film are neglected ($\nabla^2 \mathbf{m} \cong d^2 \mathbf{m} / dz'^2$). These assumptions are satisfied in experiments reported to date. Only the case of M_z and H_i even in z' is considered explicitly, although the formalism is valid for odd M_z and H_i . Adding an odd term in M_z or H_i will give nonzero intensities for the odd modes.

In Sec. II, the equation of motion of the magnetization is cast into a form appropriate for the present investigation. In Sec. III, some general information about the surface pinning is extracted from these equations without having to consider the specific functional forms of M_z and H_i in the surface region. In Secs. IV and V, two specific models for the functional form of M_z in the surface region are considered.

Portis³ has considered the effect of the variation of the saturation magnetization in the bulk region on the low-order modes. In Sec. VI, the effect on the intensities of the high-order modes (out of the Portis well) is considered. Wigen, Kooi, and Shanabarger⁴ have made numerical calculations of intensities for the case of M_z given by (1.2) with $f = (2z'/S)^2$ and with $m=0$ at $z' = \pm \frac{1}{2}S$ or $dm/dz' = 0$ at $z' = \pm \frac{1}{2}S$. Hirota⁴ numerically calculated intensities for the same M_z for the case of $m=0$ at $z' = \pm \frac{1}{2}S$.

In Sec. VII, the effect of an inhomogeneous H_i (and constant M_z) is considered. In Sec. VIII, the pinning of the modes in parallel resonance is considered, and in the Appendix, the pinning conditions of \mathbf{m} and its normal derivative at a relatively sharp discontinuity of M_z are considered. Important results are denoted by boldface parentheses around the equation number.

A preliminary report of the present investigation, which includes a brief discussion of the agreement of the theoretical results with published experimental data, has been given elsewhere.¹⁴ A more detailed report of experimental results will be given in Part V¹⁵ of the present series of papers.

¹¹ M. Sparks, second preceding paper, Phys. Rev. B 1, 3831 (1970).

¹² H. Benson and D. L. Mills, Phys. Rev. 188, 849 (1969).

¹³ V. V. Gann, Soviet Phys.—Solid State 8, 2537 (1967).

¹⁴ M. Sparks, Phys. Rev. Letters 22, 1111 (1969).

¹⁵ P. Besser and M. Sparks, Paper V of the present series of papers (unpublished).

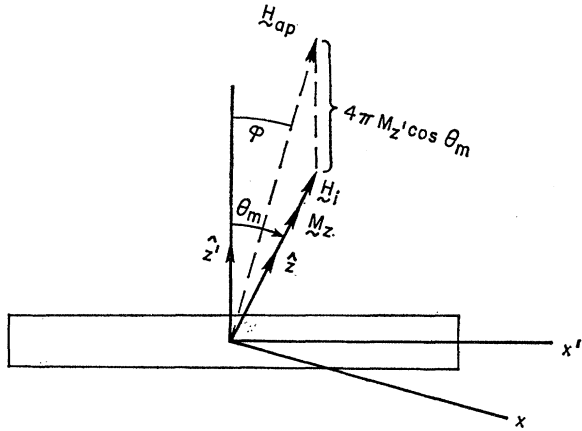


FIG. 2. Schematic illustration showing fields, angles, and coordinate systems used in the text. The axis of quantization is z , and the z' axis is normal to the film surface ($\mathbf{H}_{ap} = \mathbf{H}_{app}$).

II. EQUATIONS OF MOTION

The equation of motion of the magnetization \mathbf{M} is

$$\frac{d\mathbf{M}}{dt} = -|\gamma| \mathbf{M} \times (\mathbf{H}_i + \mathbf{h}_d + \Lambda \nabla^2 \mathbf{M}), \quad (2.1)$$

where γ is the gyromagnetic ratio, \mathbf{H}_i is the internal (demagnetized) field, \mathbf{h}_d is the microwave demagnetization field, and Λ is the exchange constant. Following Portis,³ it is assumed that Λ is independent of position \mathbf{r} . The random-phase approximation gives this result. For the case of an inhomogeneous H_i and constant M_s , the results are not affected by the assumption. For an inhomogeneous M_s , the qualitative features of the results are not effected by the assumption, but a spatial variation in Λ would affect the quantitative features. The geometries of the film and the fields are shown in Fig. 2.

The microwave demagnetization field \mathbf{h}_d was considered in detail in Part I of the present series of papers.¹¹ For the purpose of studying the pinning of the exchange modes, it is sufficient to use

$$\mathbf{h}_d = \hat{z}' 4\pi m_x \sin \theta_m, \quad (2.2)$$

which gives the correct frequencies for exchange modes in perpendicular and parallel resonance when M_z is constant. As illustrated in Fig. 2, θ_m is the angle between $\hat{z}M_z$ and the film normal \hat{z}' . The internal field \mathbf{H}_i is

$$\mathbf{H}_i = \mathbf{H}_{app} - \hat{z}' 4\pi M_z \cos \theta_m + \mathbf{H}_{an}, \quad (2.3)$$

where \mathbf{H}_{app} is the applied field, $\hat{z}' 4\pi M_z \cos \theta_m$ is the static demagnetization field, and \mathbf{H}_{an} represents the effect of anisotropy, magnetostriction, and possibly other effects.

Substituting (2.2) and (2.3) into (2.1), linearizing by neglecting the small terms $\mathbf{m} \times \mathbf{h}_d$ and $\mathbf{m} \times \Lambda \nabla^2 \mathbf{m}$, replacing $\nabla^2 \mathbf{m}$ by $d^2 \mathbf{m} / dz'^2$, using $\hat{z} \times \hat{z}' = -\hat{y} \sin \theta_m$ and $\hat{z} \times \mathbf{m} = \hat{y} m_x - \hat{x} m_y$, and assuming $e^{i\omega t}$ time dependence

gives

$$M_z \Lambda \begin{bmatrix} m_x'' \\ m_y'' \end{bmatrix} = \begin{bmatrix} H_I + 4\pi M_z \sin^2 \theta_m & -i\bar{\omega} \\ i\bar{\omega} & H_I \end{bmatrix} \begin{bmatrix} m_x \\ m_y \end{bmatrix}, \quad (2.4)$$

where $\bar{\omega} \equiv \omega / |\gamma|$, the double prime denotes d^2/dz'^2 , and^{15a}

$$H_I \equiv H_i + \Lambda M_z''. \quad (2.5)$$

For simplicity, it is assumed that the direction of \mathbf{H}_{an} is the same as that of \mathbf{H}_i and that H_{an} has been absorbed into H_i . Diagonalizing the matrix in (2.4) gives

$$M_z \Lambda m'' + \kappa^2 m = 0, \quad (2.6)$$

where m is the linear combination of m_x and m_y (e.g., $m = m_x + im_y$ in the circular precession approximation¹⁶) obtained in the diagonalization, and

$$\kappa^2 = [\bar{\omega}^2 + (2\pi M_z \sin^2 \theta_m)^2]^{1/2} - H_I - 2\pi M_z \sin^2 \theta_m \quad (2.7)$$

is the positive root of the secular equation.

This result (2.6) is the equation which will be used in the pinning study. For perpendicular resonance, $\sin^2 \theta_m = 0$ and (2.7) reduces to

$$\kappa_1^2 = \bar{\omega} - H_I = \bar{\omega} - H_i - \Lambda M_z''. \quad (2.8)$$

For parallel resonance, $\sin^2 \theta_m = 1$, and (2.6) reduces to

$$\kappa_{11}^2 = [\bar{\omega}^2 + (2\pi M_z)^2]^{1/2} - H_i - 2\pi M_z - \Lambda M_z''. \quad (2.9)$$

The effect of the volume microwave demagnetization could be included formally by solving

$$\bar{\omega}^2 = (H_I + \kappa^2)(H_I + \kappa^2 + 2\bar{\omega}_d) \quad (2.10)$$

for κ^2 . Equation (2.10) is the well-known spin-wave dispersion relation with H_i replaced by $H_i + \Lambda M_z'' \equiv H_I$ and with $Dk^2 \cong Dk_z^2 = \kappa^2$. This gives

$$\kappa^2 = [\bar{\omega}^2 + \bar{\omega}_d^2]^{1/2} - H_i - \Lambda M_z'' - \bar{\omega}_d,$$

which reduces to (2.7) when $\bar{\omega}_d = 2\pi M_z \sin^2 \theta_m$.

III. GENERAL CONSIDERATIONS OF SURFACE-LAYER THICKNESS

The thickness ϵ of the surface region is the most important single feature in determining the pinning, as discussed in the Introduction. The case of a surface layer of different M_z is particularly simple because arguments which are independent of the specific form of M_z in the surface region can be given to establish general results as follows: The thinner the boundary region, i.e., the smaller ϵ , the larger will be the exchange term $\Lambda M_z''$ in (2.7). For a sufficiently small ϵ , $\Lambda M_z''$ will be larger than the sum of the other terms in (2.7), and (2.6) reduces to

$$M_z m'' = m M_z''. \quad (3.1)$$

Integrating once with $m = M_z = 0$ at $z' = \pm \frac{1}{2}(S + \epsilon)$ (see Fig. 1) gives

$$M_z m' = m M_z'. \quad (3.2)$$

^{15a} In Paper I, H_I was defined differently.

¹⁶ M. Sparks, *Ferromagnetic-Relaxation Theory* (McGraw-Hill Book Co., New York, 1964), Sec. 3.3, p. 69.

Since the equation holds everywhere in the boundary region including $z' = \pm \frac{1}{2}(S - \epsilon)$ and m and m' are continuous, since M_z and $M_{z'}$ are assumed to be continuous, (3.2) is valid at the edge of the bulk region (denoted by B), i.e.,

$$m_B'/m_B = M_B'/M_B, \quad (3.3)$$

where M_{zB} has been written as M_B . Thus, (2.6) can be solved in the bulk region with the boundary condition (3.3) at the ends of the bulk region [at $z' = \pm \frac{1}{2}(S - \epsilon)$]. Note in particular that $M_B' = 0$ if M_z is constant in the bulk region, and (3.3) shows that $m' = 0$ at the boundary of the bulk region, i.e., the surface spins are unpinned.

The effect of the sharp surface region is to establish this boundary condition (3.3) for the bulk region. This result can be obtained also quite simply by requiring that the net additional torque on a surface spin caused by the missing neighboring spins be equal to zero for a perfectly sharp boundary ($\epsilon = 0$). The equation-of-motion method shows that the result is also valid for $\epsilon \neq 0$ as long as ϵ is sufficiently small for $\Delta M_z''$ to be larger than the sum of the other terms in (2.7) and it lifts the restriction $M_B' = 0$.

The size of ϵ below which the boundary condition (3.3) can be used in perpendicular resonance can be estimated as follows: From (2.8) with $\tilde{\omega} \cong H_{i0} + Dk_n^2$, where Dk_n^2 (with $D = \Delta M_B$) is the exchange contribution to the frequency for modes out of the Portis well,

$$k_1^2 = Dk_n^2 + H_{i0} - H_i - \Delta M_z''. \quad (3.4)$$

The maximum value of $H_i - H_{i0}$ in the surface region is $\approx 4\pi M_B$. For the first case of $Dk_n^2 \ll 4\pi M_B$, the term $\Delta M_z''$, which is of the order of $4D/\epsilon^2$ in the surface region, is larger than the other terms on the right-hand side of (3.4) when

$$\epsilon^2 \ll \Delta/\pi, \quad \text{for } Dk_n^2 \ll 4\pi M_B. \quad (3.5)$$

For the second case of $Dk_n^2 \gg 4\pi M_B$, the corresponding result is (with $k_n \equiv 2\pi/\lambda_n$)

$$\epsilon^2 \ll (\lambda_n/\pi)^2, \quad \text{for } Dk_n^2 \gg 4\pi M_B. \quad (3.6)$$

An expression which is valid in both limits is

$$\epsilon^2 \ll \epsilon_{\text{crit}}^2, \quad \epsilon_{\text{crit}}^2 = (\Delta/\pi)(1 + Dk_n^2/4\pi M_B)^{-1}. \quad (3.7)$$

More specific information on the effect of the size of ϵ on the mode intensities is given in subsequent sections where specific models of M_z and H_i are considered. The case of parallel resonance is considered in Sec. VIII.

IV. STEP-FUNCTION M_z MODEL

The case of $\epsilon^2 \ll \epsilon_{\text{crit}}^2$ satisfied will be called the *thin-surface-layer* case, that of $\epsilon^2 \ll \epsilon_{\text{crit}}^2$ not satisfied will be called the *thick-surface-layer* case, and that of $\epsilon^2 \gg \Delta/\pi$ will be called the *very-thick-surface-layer* case. In order

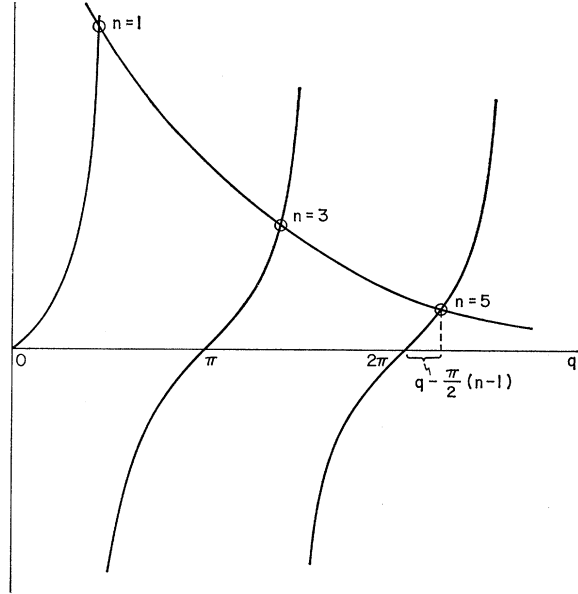


FIG. 3. Sketches of the two sides of (4.9) illustrating the numerical solution for the roots k_n of (4.9). Here, $q \equiv \frac{1}{2}k_n S$.

to calculate the pinning for the thick-surface-layer case and demonstrate the transition to the thin-surface-layer case, we consider the simple surface-layer model of a step in M_z . In the bulk region $M_z = M_B$ and in the surface region of thickness $\frac{1}{2}\epsilon$, $M_z = M_S$, where M_B and M_S are constants (see Fig. 1). The first-order effect that the modes are unpinned for a thin surface layer and that the low-order modes are pinned by a thick surface layer is independent of the specific model used. Another model for M_z will be considered in Sec. V.

The relative intensities I_n of the modes for constant ω are given by the expression¹¹

$$I_n = \frac{1}{\Delta H_n S I_{z'}} \left| \int_{-\frac{1}{2}(S+\epsilon)}^{\frac{1}{2}(S+\epsilon)} dz m(z) \right|^2, \quad (4.1)$$

$$I_{z'} = \frac{2}{S} \int_{-\frac{1}{2}(S+\epsilon)}^{\frac{1}{2}(S+\epsilon)} dz m(z)^2,$$

where ΔH_n is the linewidth of the n th resonance line. This result is valid in the circular-precession approximation.¹⁶ In general, the intensity depends upon the polarization of the microwave field used to excite the mode. For example, for a microwave field polarized along the x axis, m in (4.1) must be replaced by m_x . In the circular-precession approximation, the ratio of m_x to m is the same for all modes; thus, (4.1) gives the correct intensities. In perpendicular resonance in metallic films, the exchange modes have \mathbf{k} along the z axis, and the precession is circular. In YIG, which has a relatively small value of $4\pi M_B = 1750$ Oe (at room temperature), the precession is very nearly circular except at low frequencies (below X band).

In parallel resonance in metallic films, m_x/m can vary substantially from mode to mode, but this effect is not important in experiments performed to date, since only the first few modes are usually observed, as discussed in Sec. VIII. Thus, (4.1) is a good approximation for all modes which will be considered here. However, it should be kept in mind that the ellipticity correction, which depends on the polarization of the microwave drive field, is required, in general. For example, surface waves can have highly elliptical precession. It is possible that the coupling to both surface waves and bulk waves could give a nonsymmetrical line shape near parallel resonance.

For the odd modes, the integral in (4.1) vanishes by symmetry. In order to evaluate the integral for even modes, the functional form of m in the bulk and surface regions must be found. The solution to (2.6) in the surface region with $dm/d\zeta=0$ at $\zeta=0$ [from (3.2)], where $\zeta \equiv z' - \frac{1}{2}(S + \epsilon)$, is (for perpendicular resonance)

$$m = m_{S0} \cos k_{1S} \zeta, \quad (4.2)$$

$$k_{1S}^2 = \frac{4\pi}{\Lambda} \left(\frac{H_{iB} - H_{iS}}{4\pi M_S} + \frac{Dk_n^2}{4\pi M_S} \right).$$

For k_{1S}^2 negative, (4.2) gives

$$m = m_{S0} \cosh |k_{1S}| \zeta. \quad (4.3)$$

In the bulk region,

$$m = \left(\frac{2}{-S} \right)^{1/2} \cos k_n z. \quad (4.4)$$

Substituting (4.2) and (4.4) into (4.1) gives

$$I_n = \frac{4}{SI_z} \left| \int_0^{\frac{1}{2}\epsilon} d\zeta m_{S0} \cos k_{1S} \zeta + \int_0^{\frac{1}{2}S} dz \left(\frac{2}{-S} \right)^{1/2} \cos k_n z \right|^2.$$

Evaluating the integrals, eliminating $m_{S0} \sin k_{1S} \zeta$ by using (A4) at the interface $\zeta = \frac{1}{2}\epsilon$, and using

$$\frac{M_B}{M_S} k_n^2 - k_{1S}^2 = \frac{M_B - M_S}{M_S} \frac{4\pi}{\Lambda}, \quad (4.5)$$

gives

$$I_n = \frac{8}{(k_n S)^2 I_{z'}} \left(\frac{M_B - M_S}{M_S} \right)^2 \left(\frac{4\pi}{\Lambda k_{1S}^2} \right)^2 \sin^2 \frac{1}{2} k_n S \quad (4.6)$$

for the step function M_z . It is easy to show that this result (4.6) is also valid for negative k_{1S}^2 , i.e., for m given by (4.4) in the surface region. The value of $I_{z'}$, defined in (4.1), is typically of the order of unity.

For negative k_{1S}^2 , an alternative form of (4.6) can be obtained as follows: The logarithmic derivative of m in (4.3) evaluated at $\zeta = \frac{1}{2}\epsilon$ is

$$m_S'/m_S = |k_{1S}| \tanh \frac{1}{2} |k_{1S}| \epsilon, \quad (4.7)$$

and the logarithmic derivative of m in (4.4) evaluated at $z = -\frac{1}{2}S$ is

$$m_B'/m_B = k_n \tan \frac{1}{2} k_n S. \quad (4.8)$$

In (4.7), the subscript S denotes the limit $\zeta \rightarrow \frac{1}{2}\epsilon$ and, in (4.8), the subscript B denotes the limit $z' \rightarrow -\frac{1}{2}S$. Substituting (4.7) and (4.8) into (A5) gives

$$\tan \frac{1}{2} k_n S = A, \quad (4.9)$$

$$A \equiv (|k_{1S}|/k_n) (M_S/M_B)^2 \tanh \frac{1}{2} |k_{1S}| \epsilon.$$

Substituting (4.9) and the identity

$$\sin^2 q = \tan^2 q / (1 + \tan^2 q) \quad (4.10)$$

into (4.6) gives

$$I_n = \frac{8}{(k_n S)^2 I_{z'}} \left(\frac{M_B - M_S}{M_S} \right)^2 \left(\frac{4\pi}{\Lambda |k_{1S}|^2} \right)^2$$

$$\times \frac{(M_S/M_B)^4 (|k_{1S}|/k_n)^2 \tanh^2 \frac{1}{2} |k_{1S}| \epsilon}{1 + (M_S/M_B)^4 (|k_{1S}|/k_n)^2 \tanh^2 \frac{1}{2} |k_{1S}| \epsilon} \quad (4.11)$$

for $\Lambda k_n^2 / 2\pi \leq 1$ and the step-function M_z , with k_{1S}^2 defined in (4.5). For positive k_{1S}^2 , it is easy to show that (4.11) is valid if \tanh is replaced by \tan , which is not surprising since $|\tan^2 ix| = \tanh^2 x$.

The most interesting limiting case of (4.11) is that of $M_S = \frac{1}{2}M_B$ and

$$\tanh \frac{1}{2} |k_{1S}| \epsilon \cong \frac{1}{2} |k_{1S}| \epsilon. \quad (4.12)$$

Equation (4.12) is valid if $\frac{1}{2} |k_{1S}| \epsilon \lesssim 1$, or

$$\bar{\epsilon} (|1 - \bar{k}^2|)^{1/2} \gtrsim 1, \quad (4.13)$$

where we have introduced the convenient dimensionless parameters

$$\bar{\epsilon}^2 \equiv \pi \epsilon^2 / \Lambda, \quad \bar{k}^2 \equiv \Lambda k_n^2 / 2\pi. \quad (4.14)$$

Then, with $M_S = \frac{1}{2}M_B$, (4.11) reduces to

$$I_n = [8/I_{z'} (k_n S)^2] [(1 - \bar{k}^2) + 8(\bar{k}^2/\bar{\epsilon}^2)]^{-1} \quad (4.15)$$

for this case in which (4.13) is satisfied. From (4.15), it is seen that

$$I_n \cong \frac{8}{(k_n S)^2 I_{z'}}, \quad (4.16)$$

for $Dk_n^2 \ll \frac{1}{16} \bar{\epsilon}^2 4\pi M_B$, $Dk_n^2 \ll 2\pi M_B$, and $\frac{1}{2} |k_{1S}| \epsilon \lesssim 1$, and

$$I_n = 2\pi^2 \frac{\epsilon^2 S^2}{\Lambda^2} \frac{1}{(k_n S)^4 I_{z'}}, \quad (4.17)$$

for $\frac{1}{16} \bar{\epsilon}^2 4\pi M_B \ll Dk_n^2 < 2\pi M_B$, $\frac{1}{2} |k_{1S}| \epsilon \lesssim 1$, $M_S = \frac{1}{2}M_B$, and $\bar{\epsilon}^2 \gtrsim 1$. It is easy to show that the restriction on Dk_n^2 in (4.16) can be written as

$$n < n_{2-4}, \quad n_{2-4} \equiv (\epsilon S / 2\Lambda) + \frac{1}{2}. \quad (4.18)$$

For $\bar{\epsilon} = 1$, (4.18) reduces to the result quoted previously¹⁴

$$n_{2-4} = (1/2\sqrt{\pi})(S/\sqrt{\Lambda}) + \frac{1}{2}. \quad (4.19)$$

For $\bar{\epsilon}$ sufficiently small, only the first mode is strongly pinned. This value of $\bar{\epsilon}$ corresponds to $n_{2-4} \cong 2$ in (4.18) i.e.,

$$\bar{\epsilon} \gtrsim 5\pi^{1/2}\Lambda/S, \quad \text{no pinning.} \quad (4.20)$$

The values of k_n are determined by the roots of Eq. (4.9). These values can be obtained by sketching the functions on the two sides of (4.9). The roots correspond to the crossings of the two sets of curves. This is illustrated schematically in Fig. 3, where the crossings are denoted by circles. The resulting values of k_n are

$$k_n = (n - p_n)\pi/S, \quad (4.21)$$

where $n = 1, 2, 3 \dots$ and $0 < p_n < 1$. Figure 3 gives the value of k_n for the even modes (odd n) only. A similar figure gives values of k_n for the odd modes.

The central result of the present section, that the low-order modes are pinned by a thick surface layer, are independent of exact shape of M_z , as will be illustrated in Sec. V. For the very-thick-surface-layer case of $\bar{\epsilon}^2 > 1$, I_n drops below the fully-pinned value given in (4.16) for the step-function M_z model with $M_S = \frac{1}{2}M_B$. This reduction is model-dependent and does not occur for other shapes of M_z , as will be seen in Sec. V.

The results for large Dk_n^2 [larger than the value given for (4.17)] are model-dependent. In this case, there are many oscillations of m within the surface region. The result quoted previously¹⁴ ($I_n \sim 1/k_n^8$) for very large Dk_n^2 were obtained by neglecting the contribution to I_n from the surface region. In the present more complete treatment, there is no apparent reason for neglecting the surface-region contribution to I_n . Even though agreement with the one existing experiment can be obtained in this way, it should be emphasized that the model-dependent results indicate that the shape of M_z must be known before the pinning of the higher-order modes can be determined. Several models could be studied in detail to illuminate this point if other experimental results appear.

All of the results of this section, such as (4.11), (4.16), and (4.17), can be understood physically by sketching m in the surface and bulk regions. For example, Fig. 4

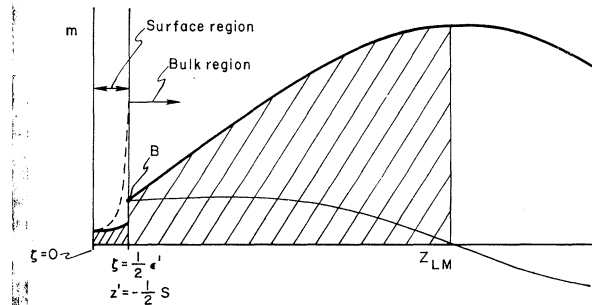


Fig. 4. Sketches of m in the surface region and adjoining portion of the bulk region used in an intuitive explanation of the results. The heavy curve is for a mode which is essentially pinned, and the light curve is for a mode which is essentially unpinned.

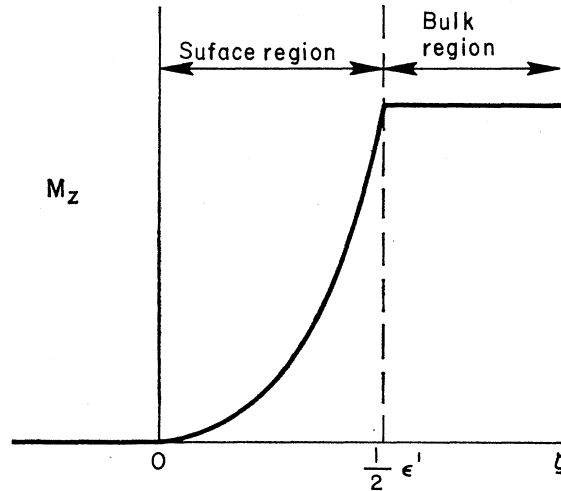


Fig. 5. Quadratic M_z in the surface region used in Sec. V as a model of M_z for which an exact solution of the equation of motion can be obtained.

is sketched for the case in which the inequalities in (4.18) and (4.13) are satisfied. The condition (4.12) means that m is rather flat in the surface region (solid curve in Fig. 4) rather than rising sharply (dashed curve). The inequality in (4.18) means that the logarithmic derivative at point B in Fig. 4 is large (heavy curve) rather than small (light curve).

In (4.1), the integral from $z=0$ to the last maximum of m (at $z=z_{LM}$ in Fig. 4) is zero since the positive and negative quarter cycles of $\cos k_n z$ integrate to zero. Thus, the net value of the integral

$$\int_{-\frac{1}{2}(S+\epsilon)}^0 dz m$$

is represented by the shaded area in Fig. 4, which is very nearly equal to the area of one-quarter of a cycle of $\cos k_n z$ [corresponding to full pinning, i.e., $I_n = 8/(k_n S)^2$]. For a very small logarithmic derivative (light line in Fig. 4), the last maximum would be at $z' \cong -\frac{1}{2}S$ (corresponding to an essentially unpinned mode).

In passing, note that for small ϵ the hyperbolic cosine in (4.3) is approximately constant. The results (A1) and (A4) show that m and M_z have the same functional form (step functions) to the left of point B in Fig. 4, in agreement with the general result of Sec. III that m has the same functional form as M_z in the surface region for a sufficiently small ϵ .

V. SMOOTHLY INCREASING M_z MODEL

In order to demonstrate explicitly which features of the step-function- M_z model of Sec. IV are model-dependent, we now consider another form for M_z in the surface region for which (2.6) can be solved analytically.

Consider the smoothly increasing function

$$M_{\text{surf}} = M_B(\zeta/\frac{1}{2}\epsilon')^2, \quad (5.1)$$

which is illustrated in Fig. 5. Substituting (5.1) into the equation of motion (2.6) and using $\tilde{\omega} \cong H_{\text{app}} - 4\pi M_B + \Lambda M_B k_n^2$ gives (for perpendicular resonance)

$$m'' + [\beta^2 - (4l^2 - 1)/4\zeta^2]m = 0, \quad \beta^2 \equiv 4\pi/\Lambda, \quad (5.2)$$

where

$$l^2 = l_\infty^2 + (\frac{3}{2})^2 - \frac{1}{4}k_n^2\epsilon'^2, \quad l_\infty^2 = \pi\epsilon'^2/\Lambda, \quad (5.3)$$

in the surface region. The solution to (5.2) for m in the surface region is (with $\frac{1}{2}\beta\epsilon' = l_\infty$)

$$m = m_B(\zeta/\frac{1}{2}\epsilon')^{1/2} J_l(\beta\zeta)/J_l(l_\infty). \quad (5.4)$$

At the surface-bulk interface, M_z is continuous, but M_z' is discontinuous; thus, (A1) and (A2) give

$$m_B = m_I, \quad m_B' = m_I' - (4/\epsilon')m_I, \quad (5.5)$$

where the subscripts B and I denote the limits $z' \rightarrow -\frac{1}{2}S$ and $\zeta \rightarrow \frac{1}{2}\epsilon'$, respectively. For

$$l_\infty^2 - \frac{1}{4}k_n^2\epsilon'^2 \equiv (\pi\epsilon'^2/\Lambda)(1 - \Lambda k_n^2/4\pi) \ll 9/4, \quad (5.6)$$

Eq. (5.3) gives $l \cong \frac{3}{2}$. And for $\pi\epsilon'^2/\Lambda \gtrsim \frac{3}{2}$, $J_{3/2}$ can be approximated by

$$J_{3/2}(\beta\zeta) \cong (\frac{1}{2}\beta\zeta)^{3/2}/\Gamma_{\frac{5}{2}}, \quad (5.7)$$

where the gamma function $\Gamma_{\frac{5}{2}} = 15(\sqrt{\pi})/8$. Equations (5.7) and (5.4) give

$$m = m_B(\zeta/\frac{1}{2}\epsilon')^2 \quad (5.8)$$

in the surface region, and (5.5) gives $m_B' = 0$. Thus, m and M_z have the same shape in the surface region when (5.7) is satisfied. This is another example of the general result of Sec. III that m and M_z must have the same shape in the surface region when the surface region is sufficiently thin.

Substituting (5.8) and (4.4) into (4.1) and evaluating the integrals gives

$$I_n = \frac{8}{(k_n S)^2 I_{z'}} (\frac{1}{6}k_n\epsilon' + \sin^2 \frac{1}{2}k_n S)^2. \quad (5.9)$$

As in Sec. IV, the factor $\sin^2 \frac{1}{2}k_n S$ can be simplified as follows: From (5.4), (5.5), and

$$\frac{d(\beta\zeta)^{1/2} J_l(\beta\zeta)}{dz} = \left[\begin{matrix} l \\ -J_l(\beta\zeta) - \beta J_{l+1}(\beta\zeta) \end{matrix} \right] \times (\beta\zeta)^{1/2} + \frac{1}{2} \left(\frac{\beta}{\zeta} \right)^{1/2} J_l(\beta\zeta), \quad (5.10)$$

it is easy to show that

$$\frac{m_B'}{m_B} = \frac{1}{\frac{1}{2}\epsilon'} \left[l - l_\infty \frac{J_{l+1}(l_\infty)}{J_l(l_\infty)} - \frac{3}{2} \right]. \quad (5.11)$$

Substituting (5.11), (4.8), and (4.10) into (5.9) gives

$$I_n = \frac{8}{(k_n S)^2 I_{z'}} \left[\frac{1}{6}k_n\epsilon' + \left(\frac{\tan^2 \frac{1}{2}k_n S}{1 + \tan^2 \frac{1}{2}k_n S} \right)^{1/2} \right]^2, \quad (5.12)$$

where

$$\tan^2 \frac{1}{2}k_n S = \frac{1}{\frac{1}{2}k_n\epsilon'} \left[l - l_\infty \frac{J_{l+1}(l_\infty)}{J_l(l_\infty)} - \frac{3}{2} \right]. \quad (5.13)$$

Equation (5.13) can be simplified as follows. From (5.3) and (5.6),

$$l \cong \frac{3}{2} + \frac{1}{3}l_\infty^2 - \frac{1}{12}k_n^2\epsilon'^2. \quad (5.14)$$

In (5.11), the following result is needed:

$$l_\infty J_{5/2}(l_\infty)/J_{3/2}(l_\infty) = \frac{1}{5}l_\infty^2, \quad (5.15)$$

for $l_\infty \gtrsim \frac{3}{2}$. Substituting (5.14), (5.15), and (5.3) into (5.13) gives

$$\tan^2 \frac{1}{2}k_n S \cong (1/\sqrt{8})(\tilde{\epsilon}/\tilde{k})(1 - \tilde{k}^2), \quad (5.16)$$

where

$$\tilde{k}^2 = (5/4)\Lambda k_n^2/2\pi, \quad \tilde{\epsilon}^2 = (16/45)\pi\epsilon'^2/\Lambda. \quad (5.17)$$

Substituting (5.16) and (5.17) into (5.12) gives

$$I_n = \frac{8}{(k_n S)^2 I_{z'}} \left[\frac{\tilde{k}\tilde{\epsilon}}{\sqrt{8}} + \left(\frac{(1 - \tilde{k}^2)^2}{(1 - \tilde{k}^2)^2 + 8(\tilde{k}^2/\tilde{\epsilon}^2)} \right)^{1/2} \right]^2. \quad (5.18)$$

It is easy to show that (5.18) reduces to (4.16) and (4.17) if $\tilde{\epsilon}$ and \tilde{k} are replaced by $\tilde{\epsilon}$ and \tilde{k} everywhere except in the factor $8/(k_n S)^2$ in (4.16) and (4.17). Thus, the two models of Secs. IV and V give the same results in the thin-surface-layer case and in the thick-surface-layer case, but not necessarily in the very-thick-surface-layer case.

Next, consider the very-thick-surface-layer case itself. For $l_\infty^2 \equiv \pi\epsilon'^2/\Lambda \geq 9/4$ and $\frac{1}{2}\tilde{k}^2 \ll 1$, it is seen from (5.3) that $l \geq (\frac{3}{2})\sqrt{2}$; thus, the small-argument expansion of J_l can be used, giving

$$m \cong m_B(\zeta/\frac{1}{2}\epsilon')^{l+1/2} \quad (5.19)$$

in the surface region. Substituting (5.19) and (4.4) into (4.1), evaluating the integrals, and eliminating m_B by using

$$m_B = \left(\frac{2}{S} \right)^{1/2} \cos^2 \frac{1}{2}k_n S = \left(\frac{2}{S} \right)^{1/2} \frac{\sin^2 \frac{1}{2}k_n S}{\tan^2 \frac{1}{2}k_n S}$$

gives

$$I_n = \frac{8}{(k_n S)^2 I_{z'}} \sin^2 \frac{1}{2}k_n S \left[\frac{\frac{1}{2}k_n\epsilon'}{(l + \frac{1}{2}) \tan^2 \frac{1}{2}k_n S} + 1 \right]^2. \quad (5.20)$$

From (4.8), (5.5), and (5.19), it follows that

$$\tan^2 \frac{1}{2}k_n S = (l - \frac{3}{2})/\frac{1}{2}k_n\epsilon'. \quad (5.21)$$

Substituting (5.21) and (4.10) into (5.20) gives

$$I_n = \frac{8}{(k_n S)^2 I_{z'}} \frac{(l - \frac{3}{2})^2}{(\frac{1}{2}k_n\epsilon')^2 + (l - \frac{3}{2})^2} \times \left[\frac{(\frac{1}{2}k_n\epsilon')^2}{(l + \frac{1}{2})(l - \frac{3}{2})} + 1 \right]^2, \quad (5.22)$$

which reduces to

$$I_n = 8/(k_n S)^2 I_{z'}, \quad \text{for } \frac{1}{2} k_n \epsilon' \ll l - \frac{3}{2}. \quad (5.23)$$

From $\pi \epsilon'^2/\Lambda \gg (\frac{3}{2})^2$, $l \cong (\pi/\Lambda)^{1/2} \epsilon'$, and (5.23) gives

$$I_n = 8/(k_n S)^2 I_{z'}, \quad \text{for } \pi \epsilon'^2/\Lambda \gg (\frac{3}{2})^2 \quad (5.24)$$

and

$$Dk_n^2 \ll 4\pi M_B.$$

It is not difficult to show that (5.24) is approximately valid for $Dk_n^2 \leq 4\pi M_B$. In particular,

$$I_n = U[8/(k_n S)^2 I_{z'}], \quad \text{for } \pi \epsilon'^2/\Lambda \gg (\frac{3}{2})^2 \quad (5.25)$$

and

$$Dk_n^2 \leq 4\pi M_B$$

where U increases from $U=1$ for $Dk_n^2 \ll 4\pi M_B$ to $U=(\frac{1}{2}\pi)^2$ for $Dk_n^2 = 4\pi M_B$.

For example, for $Dk_n^2 = 4\pi M_B$, (5.3) gives $l = \frac{3}{2}$ and $l_\infty = \frac{1}{2}\beta\epsilon' \gg 1$. Thus,

$$m \sim \cos(\beta\zeta + \pi) \quad (5.26)$$

in the surface region near the surface-bulk interface, and it is easy to show that the term $-(4/\epsilon)m_I$ in (5.5) is negligible. Thus, m and m' are continuous at the interface. The wave vector in the bulk region is $k_n = (4\pi/\Lambda)^{1/2}$, and the wave vector β in (5.26) in the surface region is also equal to $(4\pi/\Lambda)^{1/2}$. Thus, $m \sim (k_n \zeta)^{1/2} J_{3/2}(k_n \zeta)$, or

$$m = (2/S)^{1/2} (\sin k_n \zeta / k_n \zeta - \cos k_n \zeta), \quad \text{for } 0 < \zeta < \frac{1}{2}(S + \epsilon').$$

The intensity is

$$\begin{aligned} I_n &= \frac{4}{SI_{z'}} \left| \int_0^{\frac{1}{2}(S+\epsilon')} d\zeta \left(\frac{2}{S}\right)^{1/2} \left(\frac{\sin k_n \zeta}{k_n \zeta} - \cos k_n \zeta\right) \right|^2 \\ &\cong \frac{8}{(k_n S)^2 I_{z'}} \left| \int_0^\infty dx \frac{\sin x}{x} \right|^2 = \left(\frac{1}{2}\pi\right)^2 \frac{8}{(k_n S)^2}. \end{aligned}$$

This gives the stated result that $U = (\frac{1}{2}\pi)^2$.

VI. PINNING OF MODES OUT OF PORTIS WELL

Now consider the pinning of the modes out of the Portis well in perpendicular resonance by a surface layer having M_z given by (1.2) with $f = (2z'/S)^2$. With $\Delta M = 0$ in (1.2), the even solutions to (2.6) are

$$m \sim \cos k_n z, \quad k_n = (n-1)\pi/S, \quad (6.1)$$

where $n = 1, 3, 5, \dots$. With $\Delta M \neq 0$, the slope of m at the surface is no longer zero, and the shape of m differs from the pure cosine form of the unperturbed ($\Delta M = 0$) function in (6.1). The two effects will cause a shift in the value of k_n from the unperturbed values in (6.1) and an admixture of other modes into a given mode.

In order to calculate the intensities, only the admixture of the first mode $|1\rangle \rightarrow (S)^{-1/2}$ need be considered since all other modes integrate to zero. With M_z given by (1.2) with $f = (2z'/S)^2$, the equation of motion (2.6)

can be written as

$$(\mathcal{L}_0 + \mathcal{P})m = \lambda m, \quad \lambda = (\tilde{\omega} - H_{\text{app}} + 4\pi M_0)/\Delta M_0, \quad (6.2)$$

$$\mathcal{L}_0 = -\frac{d^2}{dz^2}, \quad \mathcal{P} = \frac{\Delta M}{M_0} \left(f \frac{d^2}{dz^2} + \frac{4\pi}{\Lambda} f + \frac{1}{2S^2} \right). \quad (6.3)$$

The term $1/2S^2$ in \mathcal{P} is negligible since $S^2 \gg \Lambda$. The first-order perturbation theory result for the n th eigenmode is

$$\langle z|n\rangle = \langle z|n_0\rangle + \sum_{l \neq n} \langle z|l\rangle \langle l|n\rangle, \quad (6.4)$$

where $\langle z|n_0\rangle = (2/S)^{1/2} \cos k_n z$.

The value of the coefficient $\langle 1|n\rangle$ is

$$\langle 1|n\rangle = \langle 1|\mathcal{P}|n\rangle / (\lambda_{n0} - \lambda_{10}), \quad (6.5)$$

where λ_{n0} and λ_{10} are the unperturbed values of λ for modes n and 1, respectively. For the odd modes out of the Portis well,

$$\lambda_{n0} - \lambda_{10} \cong \lambda_{n0} = Dk_n^2/\Delta M_0 = k_n^2. \quad (6.6)$$

Evaluating the integral in (6.5) and using (6.6) gives

$$\langle 1|n\rangle = 8\sqrt{2} \frac{\Delta M}{M_0} \frac{\Lambda}{(k_n S)^2} \left(\frac{4\pi}{\Lambda} - k_n^2 \right) \cos \frac{1}{2} k_n S. \quad (6.7)$$

Substituting (6.4) into (4.1) and evaluating the integrals gives

$$I_n = \frac{8}{(k_n S)^2 I_{z'}} \left| \tan \frac{1}{2} k_n S + 4 \frac{1}{(k_n S)} \frac{\Delta M}{M_0} \left(\frac{4\pi}{\Lambda k_n^2} - 1 \right) \right|^2. \quad (6.8)$$

From (4.8), (3.3), and (1.1) with $f = (2z'/S)^2$, it is easy to show that

$$\tan \frac{1}{2} k_n S = (4/k_n S) \Delta M / M_0. \quad (6.9)$$

Substituting (6.9) into (6.8) gives

$$I_n = 8(16\pi)^2 \left(\frac{\Delta M}{M_0} \right)^2 \frac{S^4}{\Lambda^2} \frac{1}{(k_n S)^8 I_{z'}}. \quad (6.10)$$

This central result shows that the intensities of the modes out of the Portis well drop off very rapidly ($I_n \sim 1/k_n^8$) in the absence of a surface-layer mechanism. Wigen, Kooi, and Shanabarger⁴ also found rapidly decreasing intensities for the modes outside the well in their computer calculations for the case of $dm/dz = 0$ at $S = \pm \frac{1}{2}S$.

VII. INHOMOGENEOUS INTERNAL FIELD

Next, consider the effect of an inhomogeneous \mathbf{H}_i for the case in which M_z is a constant. Examples of sources of an inhomogeneous \mathbf{H}_i are the demagnetization field from an imperfect surface and inhomogeneous local-strain fields.⁹

The calculations of Sec. IV still apply with only minor changes: The demagnetization field near a rough surface differs from that far away from the surface by $\sim 2\pi M_B$.⁹ Thus, $H_{iS} - H_{iB} \cong 2\pi M_B$ in (4.2). The factor $(M_B - M_S)/M_S$ in (4.6), therefore, is replaced by 1, and

(4.5) is replaced by

$$k_{1S}^2 = k_n^2 - (2\pi/\Lambda). \quad (7.1)$$

The corresponding changes in the values of I_n in (4.16) and (4.17) are

$$I_n = \frac{8}{(k_n S)^2 I_{z'}}, \quad (7.2)$$

for $Dk_n^2 \ll \frac{1}{4}\bar{\epsilon}^2 4\pi M_B$, $Dk_n^2 < 2\pi M_B$, and $\frac{1}{2}|k_{1S}| \epsilon \lesssim 1$, and

$$I_n = 8\pi^2 \frac{1}{\Lambda^2 (k_n S)^4 I_{z'}}, \quad (7.3)$$

for $\frac{1}{4}\bar{\epsilon}^2 4\pi M_B \ll Dk_n^2 < 2\pi M_B$, and $\frac{1}{2}|k_{1S}| \epsilon \lesssim 1$.

The general effect of an inhomogeneous layer of H_i is the same as that of an inhomogeneous layer of M_z ; that is, the low-order modes are pinned. Comparing (7.2) with (4.16) shows that the H_i layer pins more modes than does an M_z layer of equal thickness. That is, an inhomogeneous H_i layer is somewhat more effective than an inhomogeneous M_z layer in pinning the surface spins.

VIII. PARALLEL RESONANCE

The central feature of the experimental results for parallel resonance is that only a few, typically 1, 2, or 3 modes, are excited. This result can be understood from the step-function M_z model as follows: From (2.9) with $M_S = \frac{1}{2}M_B$,

$$k_{11S}^2 = \frac{2\pi}{\Lambda} \left\{ \left[1 + \left(\frac{\bar{\omega}}{\pi M_B} \right)^2 \right]^{1/2} - \left(1 + \frac{H_{\text{app}}}{\pi M_B} \right) \right\}. \quad (8.1)$$

Since $\bar{\omega} > H_{\text{app}}$, k_{11S}^2 is positive. Therefore, the replacements $\tanh \rightarrow \tan$, $|k_{1S}| \rightarrow k_{11S}$, and [see (4.5)]

$$\frac{M_B}{M_S} k_n^2 - k_{1S}^2 = \frac{M_B - M_S}{M_B} \frac{4\pi}{\Lambda} \rightarrow 2k_n^2 - k_{11S}^2$$

can be made in (4.11), which gives

$$I_n = \frac{8}{I_{z'} (k_n S)^2} \frac{[1 - 2(k_n^2/k_{11S}^2)]^2}{1 + 16(k_n^2/k_{11S}^2) \cot^2 \frac{1}{2} k_{11S} \epsilon}. \quad (8.2)$$

It is easy to show from (8.1) that $k_{11S}^2 > 2k_n^2$; thus, $I_n < 8(k_n S)^{-2}$. In metallic films with large values of $4\pi M_B$, the circular-precession approximation¹⁶ is usually a very poor approximation in parallel resonance.

In the extreme of very large $4\pi M_B$, (8.1) gives

$$k_{11S}^2 \simeq \frac{2\pi}{\Lambda} \left(\frac{H_{\text{app}} + 2\bar{\omega}_{\text{exc}}}{\pi M_B} \right) \ll \frac{2\pi}{\Lambda}, \quad (8.3)$$

for $4(H_{\text{app}} + \bar{\omega}_{\text{exc}}) \ll \pi M_B$.

Here $\bar{\omega}_{\text{exc}}$ is the exchange field. For example, $\bar{\omega}_{\text{exc}} = Dk_n^2$ for $M_z = \text{const}$. Then for $\bar{\epsilon}^2 \gg 1$ not satisfied, (8.2) gives

$$I_n = \frac{8}{(k_n S)^2 I_{z'}} \frac{[1 - 2(k_n^2/k_{11S}^2)]^2}{1 + 4(16)k_n^2/k_{11S}^4 \bar{\epsilon}^2}.$$

The denominator in the second factor is ≤ 2 for

$$Dk_n^2 \leq (\Lambda k_{11S}^2 / 4\pi)^2 \frac{1}{16} \bar{\epsilon}^2 4\pi M_B. \quad (8.4)$$

Since $(\Lambda k_{11S}^2 / 2\pi)^2 \ll 1$ from (8.3), comparing (8.4) with the inequality in (4.16) shows that I_n drops below the fully-pinned value of $8/(k_n S)^2$ at a much smaller value of Dk_n^2 in parallel resonance than in perpendicular resonance. In other words, many fewer modes are pinned in parallel resonance than in perpendicular resonance. Although the extreme inequality in (8.3) is not well satisfied in general, it is clear that fewer modes are excited in parallel resonance than in perpendicular resonance.

This can be demonstrated explicitly for specific cases. As an example, for 80% Ni-20% Fe permalloy, $4\pi M_B \simeq 10$ kG, and at X band $\bar{\omega} \simeq 3570$ kOe. From

$$H_{\text{app}} = [(2\pi M_B)^2 + \bar{\omega}^2]^{1/2} - \bar{\omega}_{\text{exc}} - 2\pi M_B, \quad (8.5)$$

it follows that

$$H_{\text{app}} \simeq 1144 \text{ Oe} - \bar{\omega}_{\text{exc}}, \quad (8.6)$$

and, from (8.1), the value of k_{11S}^2 is

$$k_{11S}^2 = (0.286)2\pi/\Lambda. \quad (8.7)$$

For a relatively small value of $Dk_n^2 = 375$ Oe [arbitrarily chosen to make the numerator of the second factor in (8.2) equal to $(\frac{1}{2})^2$], (8.3) gives

$$I_n = (0.05)8/(k_n S)^2 I_{z'}.$$

Thus, even the modes with the small value of $Dk_n^2 = 375$ Oe are essentially unpinned. Further reasons for the smaller pinning of exchange modes in parallel resonance than in perpendicular resonance have been discussed elsewhere.¹⁴

Finally, in the circular-precession approximation in which

$$\bar{\omega} \simeq H_{\text{app}} + Dk_n^2 + 2\pi M_B, \quad (8.8)$$

substituting (8.8) into (2.9) gives

$$k_{11S}^2 \simeq 2k_n^2 + 2\pi/\Lambda. \quad (8.9)$$

Comparison of (8.9) with (4.5) shows that (4.11) is valid if we make the replacement $k_{1S} \rightarrow k_{11S}$, $(M_B - M_S)/M_S \rightarrow \frac{1}{2}$, and $\tanh \rightarrow \tan$. Thus, (4.6) is valid if the factor of $\frac{1}{16}$ is replaced by $\frac{1}{64}$, and the modes become unpinned at a value of Dk_n^2 , which is one-fourth as large as the corresponding value for perpendicular resonance.

The results of the present section can be summarized as follows: In parallel resonance in metallic films, typically only one or two modes are strongly excited. At very high frequencies where the circular-precession approximation is more nearly satisfied, more modes may become excited. But even in the extreme limit in which the circular-precession approximation is well satisfied, fewer modes are pinned than in perpendicular resonance.

APPENDIX: CONTINUITY CONDITIONS FOR m AND ITS NORMAL DERIVATIVE AT A RELATIVELY SHARP DISCONTINUITY OF M_z

By considering the torques on the spins at a sharp interface between regions B and S having spins of

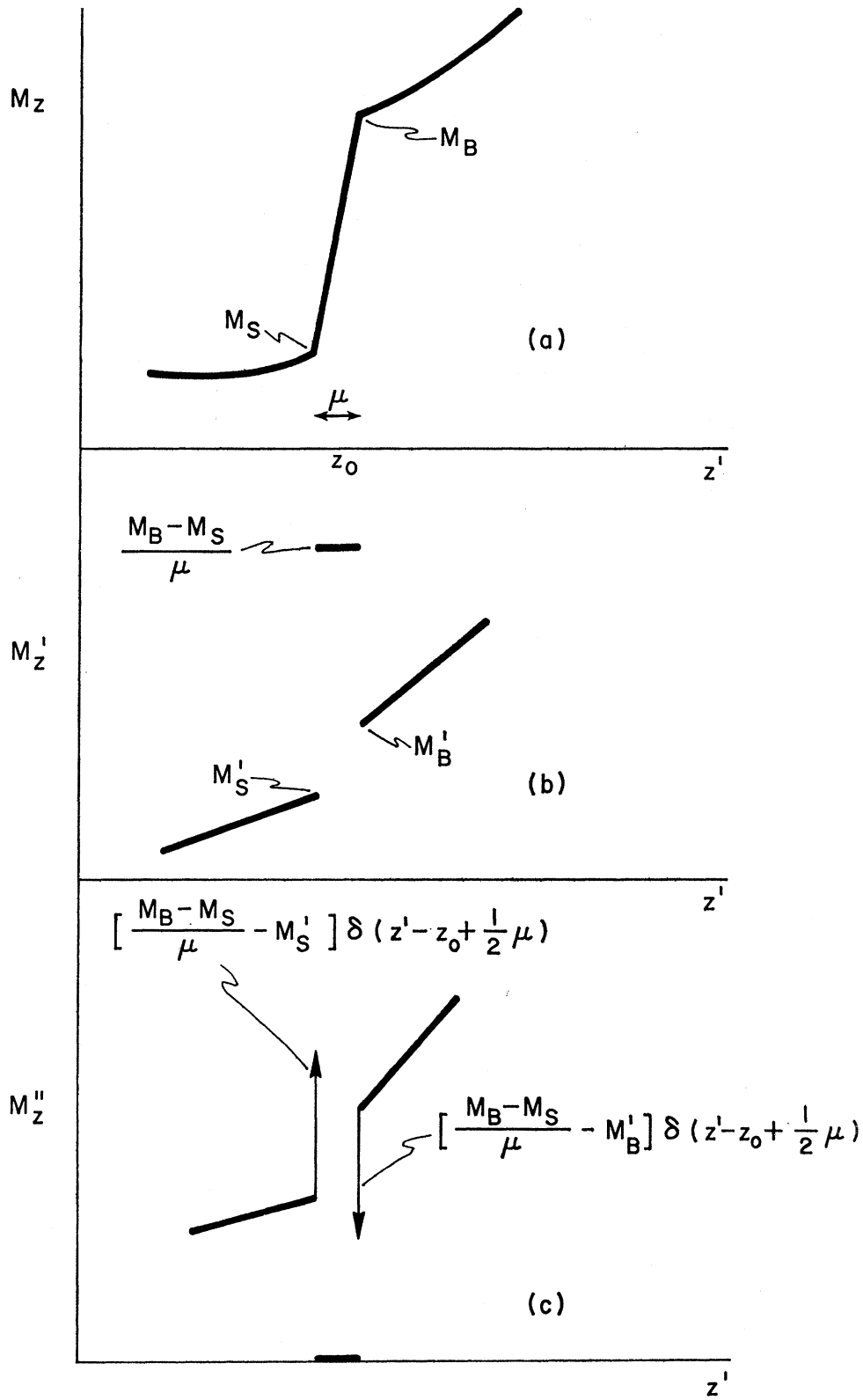


FIG. 6. Sketch of M_z and its first two derivatives showing the δ functions used in studying the continuity of m and m' at a discontinuity of M_z and/or M'_z .

different lengths (corresponding to different values M_S and M_B of M_z), it is simple to show¹⁷ in the long-wavelength limit $ka \ll 1$, where a is the lattice spacing, that

$$M_B m_S = M_S m_B, \quad (\text{A1})$$

and

$$M_B' m_B - M_S' m_S = M_B m_B' - M_S m_S'. \quad (\text{A2})$$

These results (A1) and (A2) can be obtained from the macroscopic equations of motion as follows: The derivative of a discontinuous function contains a δ function, and the second derivative of a function whose slope is discontinuous contains a δ function. The continuity conditions of a function can be studied by considering the δ functions and the derivatives of δ functions in the differential equation for the function. The terms in (2.6) which contain derivatives are

$$M_z m'' = m_S M_z'' + \text{other terms}. \quad (\text{A3})$$

Consider the case of M_z and M_z' discontinuous at some

¹⁷ M. Sparks (unpublished).

value z_0 of z' . In order to simplify the mathematics, we let M_z be continuous, but change rapidly and linearly in z' , as illustrated in Fig. 6(a). The function M_z'' contains two δ functions, as illustrated schematically in the figure. Integrating (A3) from $z_0 - \mu$ to z_0 , i.e., integrating across the first δ function in Fig. 6(c), and using the fact that m'' contains a δ function also gives

$$M_S [(m_B - m_S)\mu^{-1} - m_S'] = m_S [(M_B - M_S)\mu^{-1} - M_S'].$$

The leading terms as $\mu \rightarrow 0$ give (A1).

Integrating (A3) from $z_0 - \mu$ to $z_0 + \mu$, i.e., integrating across both δ functions, gives (A2). Note that all terms containing the factor $1/\mu$ cancelled identically.

Two results which are needed in Sec. IV are obtained from (A1) and (A2) with $M_S' = M_B' = 0$:

$$m_B' = \frac{M_S}{M_B} m_S', \quad (\text{A4})$$

$$\frac{m_B'}{m_B} = \left(\frac{M_S}{M_B} \right)^2 \frac{m_S'}{m_S}. \quad (\text{A5})$$